

Degenerate four-wave mixing spectroscopy and spectral simulation of C2 in an atmospheric pressure oxy-acetylene flame

C. F. Kaminski, I. G. Hughes, and P. Ewart

Citation: *J. Chem. Phys.* **106**, 5324 (1997); doi: 10.1063/1.473563

View online: <http://dx.doi.org/10.1063/1.473563>

View Table of Contents: <http://jcp.aip.org/resource/1/JCPSA6/v106/i13>

Published by the AIP Publishing LLC.

Additional information on J. Chem. Phys.

Journal Homepage: <http://jcp.aip.org/>

Journal Information: http://jcp.aip.org/about/about_the_journal

Top downloads: http://jcp.aip.org/features/most_downloaded

Information for Authors: <http://jcp.aip.org/authors>

ADVERTISEMENT



physicstoday

Comment on any
Physics Today article.

Physics Today / Volume 65 / Issue 7 / July 2012
Previous Article | Next Article

Measured energy in Japan
David von Seggern
(vonseg@seismo.unr.edu) University of Nevada
July 2012, page 10
DIGITAL OBJECT IDENTIFIER
<http://dx.doi.org/10.1063/PT.3.1619>

The article by Thorne Lay and Hiroo Kanamori (10.1063/PT.3.1619) is an excellent review of the energy released by the 11-Megaton hydrogen bomb test in 1952. The authors state that the energy released was approximately five times as much energy as that of a 100-megaton atmospheric nuclear detonation event—a 50-megaton nuclear device. I believe the authors used the relation for seismic energy release rather than total strain energy release. The seismic energy release by a nuclear device is a variable that depends on the fault plane. Accounting for total strain energy release would increase the earthquake energy number by orders of magnitude.

Despite the catastrophic damage potential of nuclear bombs, the forces of nature occasionally unleash much larger energy releases. Although the nuclear bombs are under our control, earthquakes, volcanic eruptions, and extreme weather events are not. However, by judicious preparation and avoidance measures, humans can significantly diminish the damage of natural events.

This article does not have any references.

Comment on this article
By the act of hitting a ball with a bat, one calculates the force energy to deliver the ball to its new location, but one must also take into account that the ball extended its energy to the strike team, which became struck by the ball as its momentum ceased and passed energy to the strike team. Therefore the parameters of the damage extend into the future when the received energy to that pushed upon, later becomes released in a new event. Perhaps calculations of one added that in while another's calculations did not. E.M.C.
Written by Edgar McCarvill, 14 July 2012 19:59

Degenerate four-wave mixing spectroscopy and spectral simulation of C₂ in an atmospheric pressure oxy-acetylene flame

C. F. Kaminski^{a)}

Lund Institute of Technology, Division of Combustion Physics, PO Box 118, S-22100 Lund, Sweden

I. G. Hughes^{b)}

Sussex Centre for Optical and Atomic Physics, University of Sussex, Brighton, BN1 9QH, United Kingdom

P. Ewart^{c)}

Clarendon Laboratory, Parks Road, Oxford, OX1 3PU, United Kingdom

(Received 21 November 1996; accepted 24 December 1996)

The $d\ ^3\Pi_g \leftrightarrow a\ ^3\Pi_u$ Swan bands of C₂ have been recorded with high resolution using DFWM in the nearly Doppler free, phase conjugate geometry. C₂ was probed in a standard oxy-acetylene welding flame with excellent signal-to-noise ratio and spectral resolution. Theoretical spectra were simulated and fitted directly to the complex overlapping spectra. The good agreement obtained shows that DFWM holds promise to become a robust and reliable tool for flame thermometry. Current theories of DFWM are reviewed in context of the present work and advantages and disadvantages of the technique are discussed. © 1997 American Institute of Physics. [S0021-9606(97)00913-6]

I. INTRODUCTION

The detection of radical species in flames and plasmas is important for the study of combustion and plasma chemistry. Furthermore, many transient species such as radicals and excited atoms or molecules can only be produced in the harsh environments of high temperature flames or electrical discharges. These environments pose experimental challenges for high resolution spectroscopy. For example the intense background emission from chemiluminescence reduces signal-to-noise ratios and the Doppler effect, arising from the high temperatures, limits spectral resolution. The process of degenerate four-wave mixing, DFWM, was demonstrated as a technique for detection of excited species and proposed as a means of probing combustion and plasma processes.¹ The detection of the OH radical in a flame was subsequently demonstrated² and DFWM has recently received much attention as a combustion diagnostic technique³ and for detection of excited molecular states.⁴

The C₂ radical is another species of interest to combustion science but is also of importance in other fields such as astrophysics and diamond synthesis using plasma assisted chemical vapor deposition. Various optical techniques have been used to study C₂ in flames.⁵ The first quantitative measurements of absolute C₂ concentrations in an oxy-acetylene flame have been reported by Baronavski *et al.*⁶ which were obtained by saturated laser induced fluorescence (LIF). Spatially resolved measurements of relative C₂ concentrations within the flame have also been reported.^{7,8} Polarization spectroscopy has recently been used to probe the C₂ (0,0) Swan bands in the oxy-acetylene torch.⁹ A recent study has

shown that spectra of C₂ in the (0,0) band could be obtained using DFWM in the forward scattering geometry.¹⁰ The spectra obtained using this geometry are subject to Doppler broadening. The use of multiplex DFWM spectroscopy of C₂, again yielding Doppler broadened spectra, has been demonstrated for single-shot temperature measurements in the oxy-acetylene flame.¹¹

In the work reported here DFWM in the phase conjugate geometry, which uses counterpropagating pump beams, was applied for the first time in the oxy-acetylene flame for the spectroscopy of C₂. The use of counterpropagating pump beams leads to a signal beam which counterpropagates with the probe and, consequently, the effective elimination of Doppler broadening provided the laser linewidth is significantly less than the Doppler width. Spectra obtained in this arrangement suffer from only a very small degree of Doppler broadening which arises owing to the finite crossing angle between pump and probe beams. The experiments described here aimed to test the feasibility of flame thermometry by DFWM spectroscopy using the C₂ radical. Ultimately the reliability of such a technique depends on its ability to predict measured spectral line shapes with high accuracy. Synthetic spectra were calculated directly and fitted to measured spectra. Current theories of DFWM are reviewed and their applicability in the context of the present work are discussed.

II. EXPERIMENT

A. Optical setup

Figure 1 shows the experimental setup used in the present work. The laser system consisted of a dye laser (Quanta Ray PDL-3) pumped by the frequency tripled output of a Nd:YAG laser (Spectron) pulsed at 10 Hz (7 ns pulse duration). To excite transitions in the $\Delta v=0$ and $\Delta v=1$

^{a)}E-mail: clemens.kaminski@forbrf.lth.se; Fax: +46 (0)46-2224542; Phone: +46 (0)46-2229728.

^{b)}E-mail: i.g.hughes@sussex.ac.uk; Fax: +44 (0)1273-678097; Phone: +44 (0)1273-678944.

^{c)}E-mail: p.ewart@physics.oxford.ac.uk; Fax: +44 (0)1865-272400; Phone: +44 (0)1865-272340.

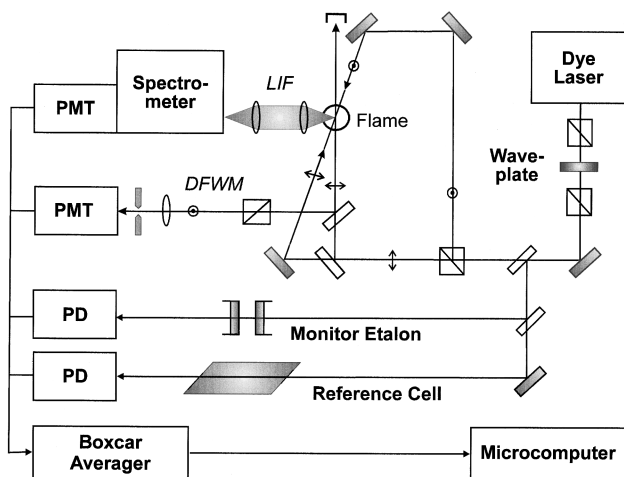


FIG. 1. Experimental layout for high resolution DFM spectroscopy of the C_2 radical. DFM was used in the Doppler free, counterpropagating geometry using polarization discrimination. PMT: photomultiplier tube; PD: photodiode.

Swan bands the dye laser was operated with methanol solutions of Coumarin 500 and Coumarin 460 laser dye, respectively. The laser beam was spatially filtered by a series of apertures arranged over a path of ~ 8 m resulting in a very homogenous intensity distribution over the entire beam diameter. The beam was passed through a double polarizer/half-wave plate assembly which allowed continuous adjustment of the laser pulse energy without introducing beamwalk. A telescope was used to reduce the beam diameter to ~ 1 mm in the interaction region.

To obtain the Doppler selectivity resulting in reduced Doppler broadening, the pump beams were arranged to counterpropagate and polarization discrimination was used to reject scattered probe and forward pump light.^{12,13} The total laser energy per pulse was typically less than $\sim 1 \mu\text{J}$ in the interaction region. The four-wave mixing signal was allowed to propagate for ~ 8 m and then spatially filtered before detection by a photomultiplier tube, PMT (Thorn EMI 9783B). This resulted in excellent discrimination of continuous chemiluminescence from the bright flame. The DFM signals from the PMT were preamplified by a low noise, fast preamplifier (EG&G Ortec VT 120) with a gain of 20 before being passed to the boxcar integrating amplifier. This increased the dynamic range of the detection system and made it unnecessary to run the boxcar amplifiers at the highest gain settings. As a result, the noise introduced by the boxcar electronics was reduced appreciably.

The interaction region was imaged by an $f/10$ optical system consisting of two lenses of 100 mm focal length and an aperture stop onto the entrance slit of a 250 mm scanning spectrograph (Hilger & Watts) employing a grating of 1800 lines per mm and equipped with a PMT. For LIF measurements the spectrograph was employed as a wide band filter to pass fluorescence and reject laser scatter. Thus, it was possible to record LIF and DFM signals simultaneously. Alternatively it was used at higher resolution in scanning

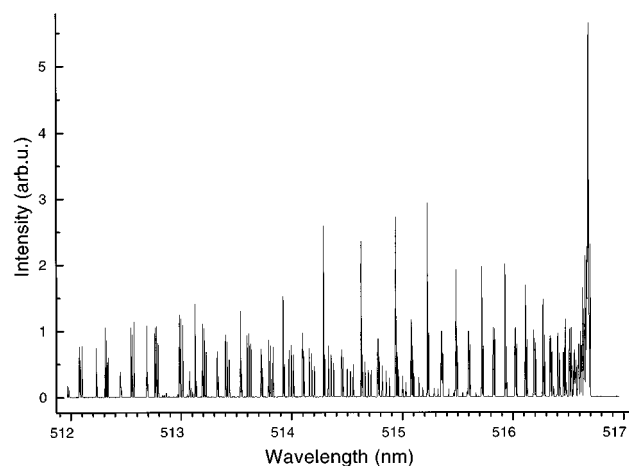


FIG. 2. High resolution DFM spectrum of the (0,0) $d^3\Pi_g \leftrightarrow a^3\Pi_u$ Swan band system of C_2 .

mode to obtain emission spectra of chemiluminescence from the flame.

For absolute wavelength calibration of the DFM spectra part of the laser energy was passed through reference absorption cells containing either I_2 vapor at room temperature or Te_2 vapor at 650°C . The DFM spectra corresponding to the $\Delta v=0$ band and the $\Delta v=1$ band of C_2 were calibrated against the reference absorption spectra using the spectral data for I_2 (Ref. 14) and Te_2 (Ref. 15), respectively. Variations in the scanning speed of the dye laser were monitored by recording fringes from a Fabry-Perot etalon (30 GHz free spectral range).

The flame used to produce the C_2 was a standard oxy-acetylene welding torch with a burner nozzle consisting of a straight copper pipe with a tapered inner bore narrowing at the exit orifice to a diameter of 1 mm. The nozzle was mounted on an $x-y-z$ translation stage to simplify positioning of the interaction region in the flame. Industrial grade acetylene and oxygen were separately fed to the burner nozzle. The flame was probed within the primary reaction zone at a height of around 4 mm above the exit plane of the nozzle. Fuel mixtures were approximately stoichiometric for all measurements presented here.

Concentration measurements of C_2 in the flame by saturated LIF have been reported.^{6,16} LIF measurements in the atmospheric flame environment are difficult to perform because of high quenching rates in the flame and the effects of partial saturation in the wings of the laser beam profile.^{17,18} The uncertainties in these measurements are correspondingly high. C_2 concentrations are generally accepted to be between 10^{12} and 10^{14} cm^{-3} for the flame operating near stoichiometric conditions.^{5,19}

III. RESULTS

Figure 2 shows a high resolution DFM spectrum covering almost the entire (0,0) $d^3\Pi_g \rightarrow a^3\Pi_u$ Swan band of C_2 . Owing to the small rotational constant of C_2 ($B \sim 1.6$

cm^{-1}) the spectrum has a high density of lines and the data demonstrate the spectral resolution afforded by DFWM. The high resolution is partly a consequence of the elimination of Doppler broadening afforded by the use of the phase conjugate geometry. The excellent signal-to-noise ratio, exceeding 400:1 near the band head, is achieved by suppressing noise arising from scatter of the probe beam from the signal beam-splitter by the polarization discrimination technique. For these reasons the technique provides an excellent tool to test the accuracy of published line positions obtained both from theory and previous experimental data which is mostly limited by Doppler broadening.

The spectrum shown is free from interferences arising from isotopic species of C_2 . The relative abundances of $^{12}\text{C}^{12}\text{C}$, $^{13}\text{C}^{12}\text{C}$, and $^{13}\text{C}^{13}\text{C}$ is approximately $1:10^{-2}:10^{-4}$, respectively (the ^{14}C isotope occurs at trace levels only). Since DFWM signals scale quadratically with species density the relative intensities of the mentioned species scale as $1:10^{-4}:10^{-8}$ and thus isotopic species are below the detection limit of the present technique. This fact simplified the interpretation and simulation of measured spectra. Assuming a C_2 concentration of 10^{13} cm^{-3} in the interaction region, we estimate a detection limit of $\sim 5 \times 10^{11} \text{ cm}^{-3}$ under the present conditions.

The staggering of successive, overlapping *P*-branch triplets towards shorter wavelength is clearly visible on the spectrum. This is a consequence of the zero nuclear spin of the molecule which means that antisymmetric levels do not occur and hence Λ doubling is absent. However, the remaining symmetric levels are affected by a Λ -type interaction and consequently the spacing between subsequent symmetric levels alternates. Since the P_1 and P_2 branches overlap strongly within their transition linewidth, this alternation leads to the observed intensity variation of the spectrum.

The *R* branch extends to shorter wavelengths from the band origin and the corresponding triplets are clearly resolved. The intensity rise towards very high *J* values visible in the *R* branch is indicative of the high temperatures present in the flame ($\sim 3000 \text{ K}$). In principle, the flame temperature could be evaluated by comparing the relative intensity of the isolated *R*-branch transitions¹⁰ using a Boltzmann plot.²⁰ However, as discussed in detail in a previous paper,¹¹ this method requires measurements over a large number of transitions to achieve temperature sensitivity, and consequently long scanning times over which it is difficult to maintain experimental stability. In the present work, overlapping high resolution DFWM spectra of C_2 were modeled theoretically for the first time. The work presented here is of direct relevance for thermometry applications based on DFWM of C_2 in combustion environments.

Figure 3 shows a comparison of a DFWM scan and a simultaneously performed LIF scan of the (1,0) band head around 473 nm. Fluorescence excited by the DFWM pump and probe beams was imaged at right angles onto the spectrometer entrance slit. Most of the resulting fluorescence ($>95\%$) is emitted into the (1,1) band near 510 nm and the rest into the (0,0) band. To capture the (1,1) fluorescence the spectrometer bandwidth was set to 12 nm centered at 512

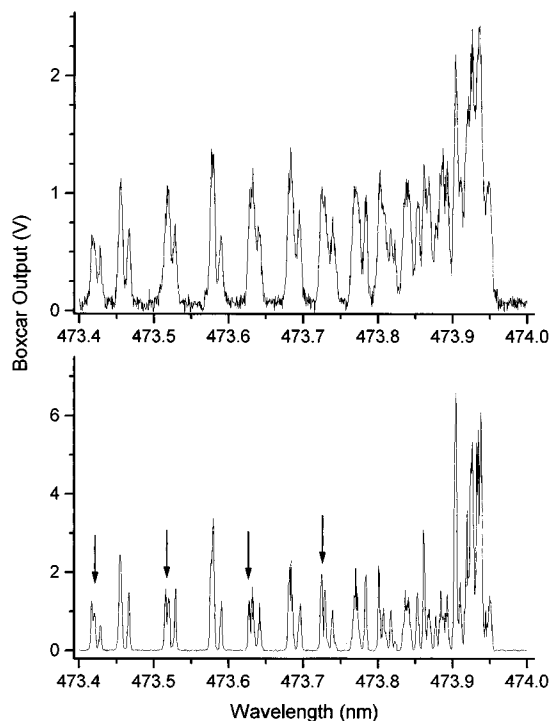


FIG. 3. DFWM spectrum of the (1,0) bands of C_2 (bottom) and LIF spectrum (top) obtained simultaneously by imaging the fluorescence excited by the probe and pump beams in the interaction region. The lower spectral resolution and signal-to-noise ratios afforded by LIF in the flame environment are evident.

nm. Signal intensities at each wavelength position correspond to the average of ten laser shots. It is evident that much of the spectral detail revealed by DFWM is lost in the LIF spectra. For example, the doublets marked by arrows on the lower spectrum are clearly resolved by DFWM but not by LIF. Note also the much higher signal-to-noise ratio afforded by DFWM. No averaging was performed between adjacent wavelength positions (“moving average”) to remove spectral noise on either of the two spectra. The noise on the LIF spectra arises mostly from intense chemiluminescence from the bright flame which competes with the LIF signals. This effect can be reduced by gating the photomultiplier voltage or using a mechanical chopper.¹¹ Neither method was attempted for the present work.

A. DFWM line shapes

A full theory of DFWM must treat effects of atomic motion, level degeneracies, spectral properties of practical laser systems used, saturation, absorption, and other effects. At present, no fully comprehensive and quantitative theory of DFWM interactions is available to properly account for these effects in all intensity and bandwidth regimes. Further theoretical and experimental investigations are required to realize the full potential of DFWM as a diagnostic probe. The C_2 radical offers an ideal test case for current theories of DFWM because it occurs naturally in many flame environments and because it has a strong oscillator strength. Furthermore, its spectrum lies in a wavelength region which is eas-

ily probed by standard dye laser systems without the requirement of nonlinear frequency mixing schemes.

The simplest and most widely applied theory of DFWM was developed by Abrams and Lind²¹ and treats the interaction of a monochromatic laser field with stationary two level absorbers (referred to hereafter as AL theory). The AL theory has been extended to include effects of atomic motion and this is known as the “moving absorber” theory.²² Again only monochromatic light fields are considered. Analytic solutions for this theory can be obtained in two extreme limits.²³ In the “infinite Doppler limit,” for radiation of wave vector k_0 , the inhomogeneous linewidth Γ_d exceeds the homogeneous width Γ , where $\Gamma_d = k_0 v_p$, and v_p is the most probable molecular speed, i.e., $\Gamma/k_0 v_p \ll 1$. In this case the theory predicts a Doppler-free Lorentzian line shape. This is because only the zero velocity class couples effectively to incident and generated fields. In the other extreme, $\Gamma/k_0 v_p \gg 1$, the homogeneous linewidth dominates (due to collisions and/or saturation broadening). In this limit the theory predicts the same Lorentzian cubed line shape as the standard AL theory. Doppler broadening and saturation effects on three and four level systems have been considered theoretically^{24,25} and experimentally.²⁶ For most practical cases these analytical theories represent extreme approximations. Recently, the situation where collisional and Doppler widths are comparable and fields are saturating has been treated theoretically by numerical integration of the density matrix equations governing the interaction.²⁷

For simulation of entire spectra, a simple analytical formula is desirable although in molecular spectra the complexity of multiple levels needs often to be considered. Multi-level effects such as coherence gratings²⁸ and crossover resonances²⁹ can give rise to subtle effects on recorded spectra. The former are a consequence of coherences set up between individual magnetic sublevels (“Zeemann coherences”) and their effect is strongly dependent on the relative polarizations of incident laser fields. They are not, however, important in the present atmospheric pressure environment where such coherences are rapidly destroyed by molecular collisions.

In NO so-called “crossover resonances” have been shown to affect dramatically the spectral appearance of DFWM scans in the γ bands.²⁹ These occur if two distinct transitions which share a common level overlap within their Doppler width. Again, the effect exhibits strong polarization dependencies and has to be taken into account even if the overlapping lines are not resolved. This effect occurs in NO because the lower Π state is Λ doubled whereas the upper Σ state is not.³⁰ There is, however, a fine splitting of each rotational level in the upper state due to a spin-rotation interaction which leaves the parity of the split levels unchanged. Since transitions to *both* of these levels are allowed by electric dipole selection rules from a given lower level, crossover resonances may occur if the spin rotation splitting is less than the Doppler width. Since in C_2 both the $d^3\Pi_g$ and $a^3\Pi_u$ states are affected by a Λ -type interaction, no transitions occur which share a common level and which overlap within the Doppler width. Crossover resonances of the type

observed in NO (Ref. 29) hence do not affect the spectrum in the present case.

Williams *et al.* have pointed out recently that the AL theory neglects contributions to DFWM signal intensities which arise from orientation and alignment effects induced by the incident laser fields in both weak³¹ and strong field limits.³² A related study has recently been carried out in the case of strong field excitation.³³ These effects depend on the geometry of the setup used (phase matching configuration) and, in particular, on the relative polarization orientation of the incident fields. This geometrical factor is J dependent but very rapidly levels out to a constant value for higher J values ($J > \sim 3$ in the present case).³¹ Importantly for spectra that encompass several rotational branches, it was shown that the relative strength between individual branches may be affected by a particular experimental geometry. In the present case only P and R branches appear in recorded spectra and for the arrangement used the geometrical factors can be shown to be the same for both branches leaving their relative strength unaffected.³¹

The bandwidth of pulsed dye lasers used for DFWM in most practical situations is comparable to, or exceeds, the homogeneous width of probed transitions. The stationary and moving absorber theories are strictly valid only for monochromatic laser fields. For laser bandwidths exceeding all molecular relaxation rates, the signal dependence on laser intensity and bandwidth has been considered theoretically³⁴ and studied experimentally.³⁵ Theoretical DFWM signal line shapes in this very broad bandwidth regime have also been calculated and compared with experimentally measurements on OH in a methane-air flame.³⁶ The theory has implications for multiplex DFWM spectroscopy where large bandwidth sources are employed to excite a number of transitions simultaneously.¹¹ In a study of the saturation behavior of DFWM in CH, this broadband theory was found to give predictions in better quantitative agreement with experiment than the monochromatic theory.³²

Although the homogeneous linewidth Γ of C_2 is not accurately known for the flame environment in the present work, it is probably less than, or of the same order as, the laser linewidth which is well represented by a Lorentzian line shape with a width of 0.11 cm^{-1} . The present case represents therefore a regime which falls within neither of the limits defined by monochromatic and very broadband lasers. Indeed, this is the situation most commonly encountered in practice. The treatment of finite but narrow laser bandwidths in DFWM is a problem that needs to be addressed in the future.

It is interesting to note, however, that in many instances where fields were used which were neither truly monochromatic or very broadband in comparison to Γ measured line shapes were very well described by the standard AL theory. These include studies in NO (Ref. 12), flame studies of OH (Refs. 23 and 20), and CH in an oxy-acetylene flame.³⁷ Furthermore, measured DFWM linewidths may be narrower than the linewidth of the laser used and this is explained by the nonlinear intensity dependence of the DFWM signal in the low intensity regime.³⁷

Below the saturation intensity I_{sat} the line shape of the DFWM signal in the AL theory is given by

$$I_c \propto \alpha_0^2 \frac{1}{1 + \delta^2} L^2 \frac{I^3}{I_{\text{sat}}^2} = CN^2 \frac{1}{(1 + \delta^2)^3}, \quad (1)$$

where the center line intensity C is given by

$$C \propto \mu_{12}^8 T_1^2 T_2^4 I^3 (I \ll I_{\text{sat}}). \quad (2)$$

Here I_c is the DFWM signal intensity, I is the laser intensity, $\delta = \Delta T_2$ is the detuning Δ from resonance normalized by the coherence decay time T_2 , α_0 is the line-center absorption coefficient, L is the interaction length, N is the population of the lower level (the upper state is essentially unpopulated in C_2 at flame temperatures), μ_{12} is the transition dipole moment, and T_1 is the population loss time. Equation (1) corresponds to a Lorentzian cubed line shape with a full width at half maximum (FWHM) given by $\Gamma_{\text{FWHM}} = \Gamma(2^{1/3} - 1)^{1/2} \sim 0.5\Gamma$, where Γ is the FWHM of the corresponding Lorentzian. I_{sat} is given by

$$I_{\text{sat}} = \frac{\hbar^2 \epsilon_0}{2T_1 T_2 |\mu_{21}|^2}. \quad (3)$$

For expressions (1) and (2) to be valid, the laser intensity must satisfy $I \ll I_{\text{sat}}$. The sensitivity of the signal intensity to that of the incident laser intensity, and its high order dependence on collisional relaxation rates and on μ_{12} , require accurate knowledge of these parameters if quantitative information is to be extracted from recorded DFWM spectra. The situation is relaxed if one works in the fully saturated regime where the signal becomes quadratically dependent on μ_{12} and independent of laser power and collisions.²² However, full saturation is difficult to achieve throughout the interaction volume and power broadening impairs resolution for intensities which greatly exceed I_{sat} . The present work was therefore conducted in the unsaturated regime.

The dependence of I_c on laser intensity was verified by monitoring, as a function of laser power, the line-center signal strength from the isolated R_3 ($J''=9$) transition (notation follows Ref. 38). The result is shown in Fig. 4. Laser energies were adjusted by the calibrated waveplate-polarizer assembly. Each point corresponds to the average of 250 single shots. A straight line fit through the first 4 points of the graph yields a slope of 3.04 ± 0.11 , but at higher laser intensities I_L the signal deviates from an I_L^3 dependence indicating that partial saturation is present. The laser power was not calibrated absolutely but an order of magnitude estimate for I_{sat} can be obtained from Eq. (3). Assuming that the population decay time and the coherence decay time are related as $2T_1 = T_2$ (Ref. 39) and assuming a homogeneous width of 0.1 cm^{-1} we estimate a line-center saturation intensity of $\sim 0.3 \mu\text{J}$ per laser pulse in the present configuration. The calculation is based on a transition dipole moment calculated from lifetime measurements.⁴⁰

The highest signal to noise ratios in DFWM are obtained when $I \approx I_{\text{sat}}$. This exploits the large increase of the signal intensity with laser power in the unsaturated regime. At intensities $I \gg I_{\text{sat}}$ noise from scattered probe light increases

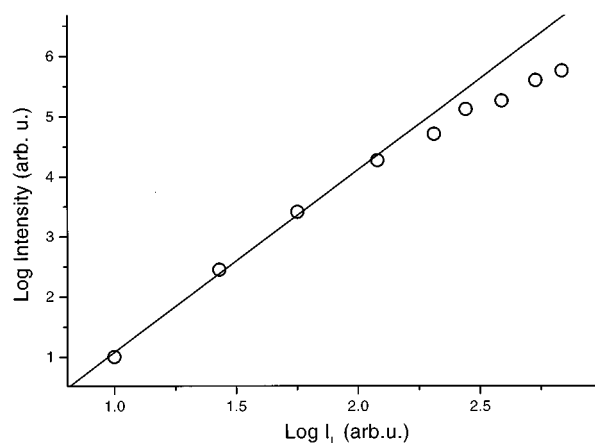


FIG. 4. Saturation behaviour of DFWM signal. A straight line fit through the first 4 points yields a slope of 3.04 ± 0.11 . For higher laser intensities partial saturation behavior is evident.

much faster than the DFWM reflectivity thus reducing the overall signal to noise ratio.³⁷ The experiments were therefore performed with laser energies just below the point where the lines began to broaden.

Since only low intensities were required, the dye laser beam, which had a diameter at the exit plane of the laser of approximately 5 mm, could be spatially filtered with relatively small apertures of 1.5 mm diameter. This reduced the overall intensity substantially but yielded a very uniform circular Gaussian intensity profile. This resulted in excellent shot to shot stability of the DFWM signals.

To investigate whether the stationary absorber theory applied in the present case, theoretical line shapes were fitted directly to isolated triplets in the R branch. The result is shown in Fig. 5. For this measurement the laser stepsize was reduced to 0.01 cm^{-1} to scan slowly over the isolated $R_1(15)$, $R_2(14)$, $R_3(13)$ transitions, respectively. The solid line fit corresponds to Lorentzian cubed line shapes repre-

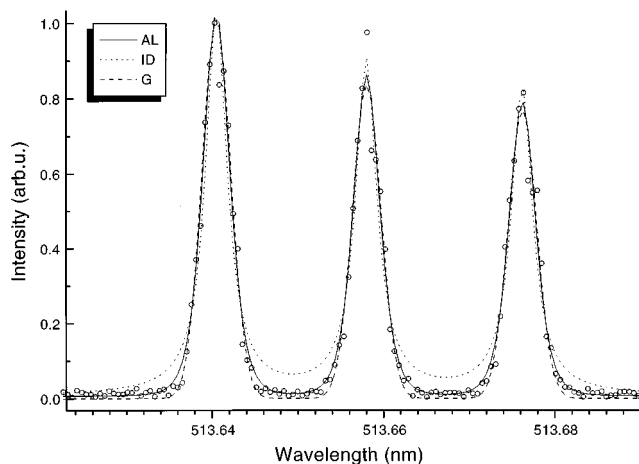


FIG. 5. Theoretical fits to line shape measurements of the $R_1(15)$, $R_2(14)$, and $R_3(13)$ transitions. Legend: AL: Abrams-Lind stationary absorber theory; ID: Moving absorber theory in the infinite Doppler limit; G: Gaussian line shape function (included for comparison).

senting the standard stationary absorber theory. Also shown is a Lorentzian fit corresponding to the moving absorber theory in the infinite Doppler limit and a Gaussian fit which is included for comparison. It is clear that the moving absorber theory, in the limit where the Doppler width far exceeds the homogeneous widths, does not apply in the current case. The Lorentzian line shape corresponding to this situation overpredicts the intensity in the extreme wings. The Gaussian profile, on the other hand, decreases too rapidly towards the wings. Clearly, the best fit occurs for the Lorentzian cubed line shape. The only fitting variable in the calculation was a single width parameter Γ_{FWHM} for all three transitions. The best fit corresponds to a linewidth $\Gamma_{\text{FWHM}}=0.12 \text{ cm}^{-1}$. This is significantly lower than the Doppler width of the C_2 molecules in the flame which is $\sim 0.16 \text{ cm}^{-1}$ ($T=3000 \text{ K}$). The residual linewidth is due to the combined effects of the laser linewidth (0.11 cm^{-1}), the homogeneous linewidth, and a residual Doppler component arising from the finite beam crossing angles. In principle the homogeneous linewidth of the transition could be extracted from such a fit if a laser source of bandwidth $\Delta\nu \ll \Gamma_{\text{FWHM}}$ is available.²³

A linewidth measurement by Doppler-free polarization spectroscopy of C_2 , using a laser linewidth of 0.05 cm^{-1} , has been reported⁹ where it was stated that, since the flame environment is predominantly collision broadened, little can be gained in spectral resolution by the use of Doppler free techniques.¹⁰ The measurement yielded a homogeneous width of 0.14 cm^{-1} which is larger than the overall linewidth of the present measurement which was performed with a laser of almost twice the linewidth. However, the previous measurement⁹ was performed under partially saturated conditions and on spectrally overlapping lines. The results presented here, on the other hand, demonstrate that Doppler free, phase conjugate DFWM offers a significant improvement in resolution compared to Doppler limited techniques.

Knowledge of the exact line shape is crucial for the synthesis of the highly overlapping spectra. In all fits performed and discussed in the subsequent sections, a Lorentzian cubed line shape was used with a single width parameter for all transitions. This procedure was justified since no linewidth variations as a function of J were evident over the entire range of recorded spectra.

B. Line positions and dependence on dipole transition moment

Knowledge of the exact line positions is also crucial for the successful simulation of complex overlapping DFWM spectra. Since line shapes add coherently small errors in the line, positions can lead to large deviations between measured and simulated spectra. Although C_2 spectroscopy has been a subject of interest for almost two centuries⁴¹ it was not until very recently that accurate data of line positions has become available. The first extensive spectral assignment has been undertaken by Phillips *et al.*⁴² but, although very comprehensive, these data are of limited accuracy and do not agree well with more recent measurements performed with more ad-

vanced equipment. The most recent measurements on the (0,0) bands have been carried out by Amiot,³⁸ Suzuki *et al.*,⁴³ and Prasad *et al.*⁴⁴ These represent the most precise measurements on C_2 line positions to date. In the present work, the Hamiltonian matrix elements presented by these authors^{38,43,44} were combined and used as input to the computer program Hund A developed by Brown *et al.*⁴⁵ This program is based on the Hamiltonian formalism developed by Brown and Merer⁴⁶ which diagonalizes upper and lower state Hamiltonian matrices of the transitions using a basis set in the Hund's case *a* representation. Agreement between the calculated line positions and the literature values^{38,44} was excellent around the band origin, although slight discrepancies were found toward high J values. The alternation in the splitting of successive P_1 and P_2 transitions was calculated to be slightly larger resulting in a larger intensity alternation in simulated spectra which better represented the measured spectra.

The program was also used to calculate accurate term energies $F(J)$ and transition strength S_{21} which were related to transition dipole moments μ_{21} . Equation (2) shows a $|\mu|$ ⁸ dependence on the line strength in the unsaturated regime. Rotational line strengths may vary significantly as a function of J in diatomic molecules and therefore the exact dipole dependence is a crucial parameter in the spectral synthesis.

Except for very low J values the Hönl–London factors calculated by Hund A (which takes intermediate coupling cases fully into account) were in excellent agreement with analytical expressions first derived by Budó for C_2 (Ref. 47). Budó's values were calculated assuming Hund's coupling case *b* which is very rapidly approached for higher J 's in C_2 . For example, in the *P* branch the transition from Hund's case *a* to case *b* is already completed for $J \geq 5$ (Ref. 44). Spectra simulated using Budó's line strength values were identical in shape to those based on Hund A calculations.

Figure 6 shows normalized plots of $|\mu_{21}|$ ⁸ and $|\mu_{21}|$ ² for the P_1 and R_1 branches in C_2 corresponding to the AL theory in the limits $I \ll I_{\text{sat}}$ and $I \gg I_{\text{sat}}$, respectively. Although the behavior is different in the two intensity regimes, the absolute variation in μ is small as a function of J in either case. This is in contrast to results obtained for NO (Ref. 48) and consequently C_2 DFWM spectra are much less sensitive to the exact dipole dependence.¹¹ Because $I \ll I_{\text{sat}}$ in this work a $|\mu|$ ⁸ dependence was assumed in the synthesis. It is worth noting that this same dipole dependence is obtained for $I \ll I_{\text{sat}}$ using the broad bandwidth theory.³⁴

Equation (1) shows how DFWM spectra are affected by the relaxation times T_1 and T_2 in the unsaturated regime. Assuming $T_1 = 2T_2 = T_r$, there is a sixth order intensity dependence on T_r for $I \ll I_{\text{sat}}$. The signal becomes independent of T_r under fully saturated conditions.²² In the present case T_r was assumed to be independent of J . Although the exact J dependence of T_r was not known, this assumption was encouraged by the fact that the measured linewidths did not change over the entire range of J values probed.

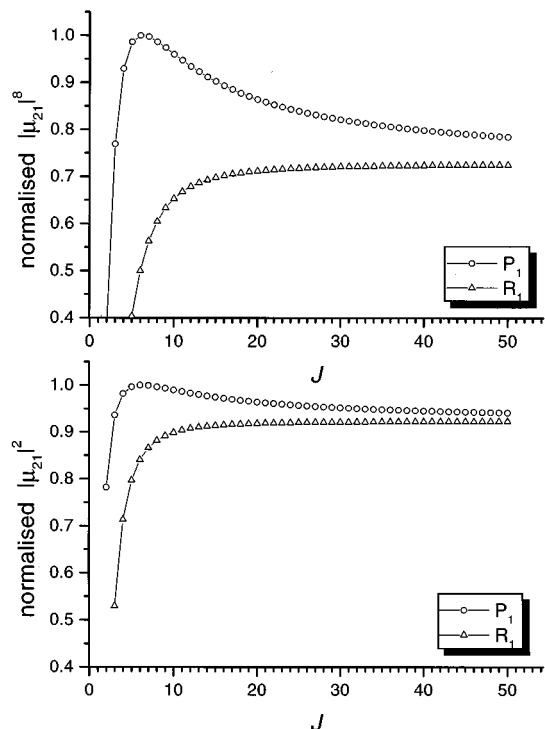


FIG. 6. Dipole dependencies of C_2 DFWM signal as a function of J'' for $I \leq I_{\text{sat}}$ ($|\mu|^8$) and $I \geq I_{\text{sat}}$ ($|\mu|^2$).

C. Spectral fitting

Figure 7 shows a theoretical fit to a DFWM spectrum recorded near the origin of the (0,0) band. The calculated line positions are indicated on the top graph. The spectrum was calculated using Lorentzian cubed line shapes with a linewidth (FWHM) of 0.12 cm^{-1} corresponding to the linewidth measured earlier and the good agreement between theoretical and experimental spectrum is apparent, despite the heavy spectral overlapping.

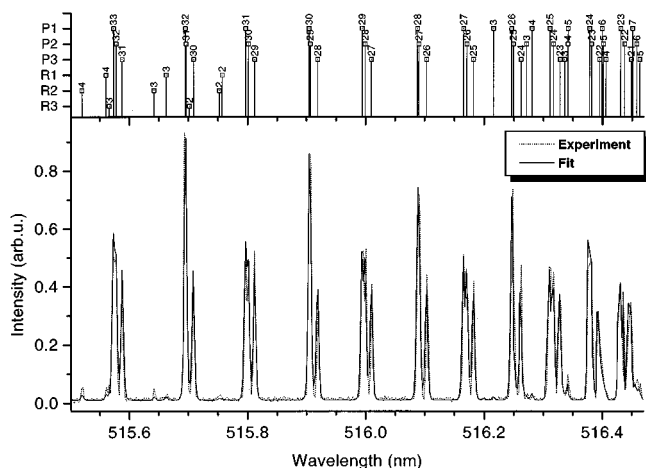


FIG. 7. DFWM spectrum near the band origin in the (0,0) band and theoretical fit. The top graph identifies line positions used in the calculation. The temperature was fixed at 3000 K for the fit.

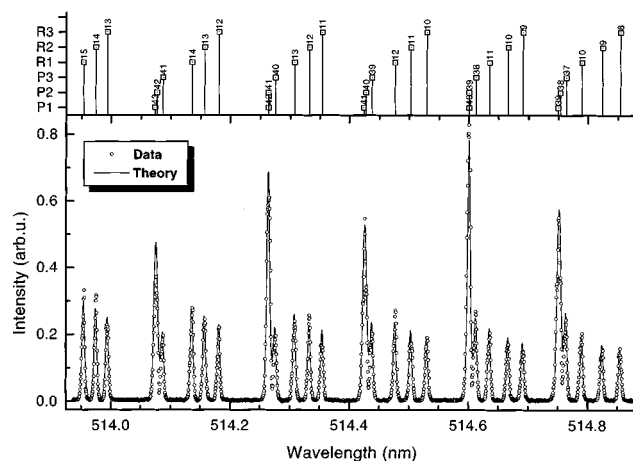


FIG. 8. Theoretical fit to a DFWM spectrum covering a temperature sensitive region. The best fit theoretical temperature corresponds to 3083 K.

In the simulation the temperature was fixed at $T=3000$ K in agreement with the expected temperature.¹¹ Near the band origin the spectral shape changes only slowly as a function of T and the exact temperature is not crucial for a good fit. For thermometry therefore a more sensitive spectral region has to be selected. In thermal equilibrium the ground state population density $N=N(J)$ in Eq. (1) follows a Boltzmann distribution:

$$N(J) = \frac{N_t}{Q_r} g_J e^{-F(J)hc/kT}, \quad (4)$$

where N_t is the total population, Q_r is the rotational state sum, g_J is the degeneracy, and $F(J)$ is the energy of the rotational level J concerned. Because of the exponential character of Eq. (4) accurate knowledge of $F(J)$ is crucial. In the present work the values of $F(J)$ were calculated directly using the Hund A program.

For thermometry applications using C_2 , spectra covering both high and low J values are required to give good temperature sensitivity over a spectral range which can be scanned in a comparatively short time. The suitable regions for C_2 thermometry have been discussed in a previous publication and in particular their suitability for single shot multiplex thermometry.¹¹ Figure 8 shows a DFWM spectrum from such a spectral region obtained by scanning the narrow linewidth laser. Each measurement point corresponds to the average of 20 laser shots. The solid line corresponds to a theoretical fit using the stationary absorber theory. The strong intensity alternation of successive, overlapping P_1, P_2 transitions is apparent and the simulated spectrum depends critically on exact linepositions. The temperature, T , was used as a floating variable to obtain the best fit theoretical spectrum yielding a temperature $T=3083$ K. This is in agreement with the accepted flame temperature⁵ for the conditions given. The good agreement between the simulated and experimental spectrum shows the potential of the technique as a reliable tool for temperature diagnostics. The signal-to-

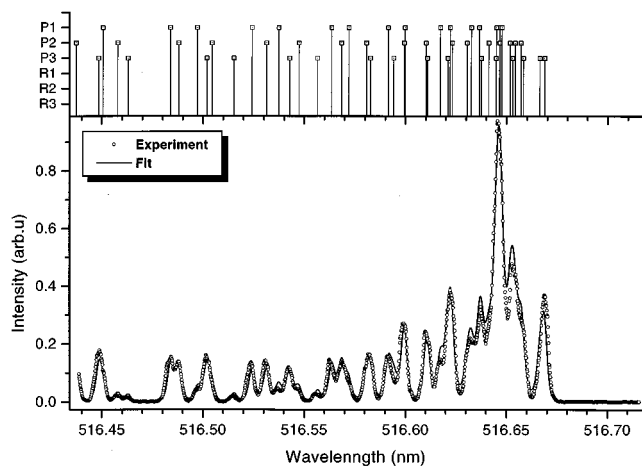


FIG. 9. High resolution DFWM spectrum of the (0,0) band head plus theoretical fit.

noise ratio on the experimental spectrum exceeds 500:1 and demonstrates the ability of the technique to probe trace species in highly luminous environments.

A subtle but interesting feature of the recorded spectra is that some of the *P*-branch lines appear to be slightly better resolved in the experimental data than in the theoretical spectra. As noted above the coherent addition of blended lines, such as those in the *P* branch, depends critically on the relative position of the components and coherent addition can, in principle, lead to interference effects depending on the relative detuning of component lines and the dephasing rate. The latter type of interference effects has not been included in the present calculations since the line positions are not known to sufficient precision and the dephasing rate, at atmospheric pressure, is sufficiently rapid to wash out such effects in most cases. However, it is possible that such an effect may lead to dips in the resultant intensity between closely spaced lines which are not included in the present theory. Overall, the temperature is found not to be dependent on the precise line shape and is sensitive more to the ratios of peak heights of the *P* and *R* branch lines.¹¹

Finally, Fig. 9 shows a fit to a high resolution spectrum obtained near the band head of the (0,0) band. Simulation of such highly overlapping spectra provides an excellent test ground for current DFWM theories. Spectral fitting to isolated lines and composite features involving crossover resonances have been reported^{27,29} and also simulations using the moving absorber model of entire DFWM spectra.⁴⁹ In the present work, the simulation covers a wide range including complex overlapping spectra where the line shape is a crucial parameter. For the calculation *T* was fixed at 3000 K. Again, the line shapes were calculated according to the stationary absorber model which was earlier found to give the best description of isolated lines. Agreement between theory and experiment is found to be excellent. These results show successful fitting of synthetic spectra to complex, highly overlapping DFWM spectra which has not been previously reported. They show the potential of DFWM to become a

diagnostic tool as robust and reliable as established techniques, such as CARS or LIF.

IV. CONCLUSIONS

This paper has presented high resolution DFWM spectroscopy of the C_2 radical obtained from a standard oxy-acetylene welding flame. DFWM was applied in the Doppler free, phase conjugate geometry. Polarization discrimination was effectively employed to reduce probe and pump scatter from flame particulates and optical components. The coherent nature of the process makes it easy to reject incoherent background luminescence from the intensely bright flame, and the resulting spectra exhibited excellent signal-to-noise ratios. These features make DFWM ideally suited to probe this harsh environment. Its advantages over LIF in this environment were highlighted since LIF suffers from effects of quenching collisions, Doppler broadening, and background emission.

DFWM spectra of C_2 were modeled theoretically for the first time and fitted to experimental data. The two level theory of Abrams and Lind, despite its approximations, serves very well to explain the observed spectral line shapes. In the present case C_2 was chosen as an ideal test species to test the potential of DFWM for flame thermometry. The accurate synthesis of C_2 spectra will allow the use of DFWM to infer temperatures in many hostile environments where this important radical occurs. Since C_2 is present in most environments where the combustion cycle of hydrocarbon fuels is incomplete, this technique shows great potential as a thermometry probe.

Line positions and transition strength were calculated directly for C_2 and slight discrepancies with published line positions were found at high *J* values. Accurate line data are crucial for a successful simulation of C_2 spectra, especially if coherent techniques are used where overlapping lines may interfere constructively. The high signal-to-noise ratio afforded by DFWM and its sub-Doppler resolution in the counterpropagating geometry show that it could serve as an alternative tool to provide accurate spectroscopic data on short lived radicals. Many radicals are created in highly luminous environments where conventional methods are limited by poor signal-to-noise ratios and Doppler broadening.

ACKNOWLEDGMENTS

I.G.H. is grateful to British Gas plc for financial support and P.E. is grateful to the Royal Academy of Engineering and British Gas plc for the award of a Senior Research Fellowship.

¹P. Ewart and S. V. O'Leary, *J. Phys. B At. Molec. Phys.* **17**, 4609 (1984).

²P. Ewart and S. V. O'Leary, *Opt. Lett.* **11**, 279 (1986).

³R. L. Farrow and D. J. Rakestraw, *Science* **257**, 1894 (1992).

⁴P. H. Vaccaro, in *Resonant Four Wave Mixing Spectroscopy: A New Probe for Vibrationally Excited Species*, edited by C.-Y. Ng (World Scientific, Singapore, 1995).

⁵A. G. Gaydon and H. G. Wolfhard, *Flames, Their Structure, Radiation and Temperature* (Chapman and Hall, London, 1979).

⁶A. P. Baronavski and J. R. McDonsald, *Appl. Opt.* **16**, 1897 (1977).

⁷M. Aldén, H. Edner, and S. Svanberg, *Appl. Phys. B* **29**, 93 (1982).

⁸M. G. Allen, R. D. Howe, and R. K. Hanson, *Opt. Lett.* **11**, 126 (1986).

- ⁹K. Nyholm, M. Kaivola, and C. G. Aminoff, *Appl. Phys. B* **60**, 5 (1995).
- ¹⁰K. Nyholm, M. Kaivola, and C. G. Aminoff, *Opt. Comm.* **107**, 406 (1994).
- ¹¹C. F. Kaminski, I. G. Hughes, G. M. Lloyd, and P. Ewart, *Appl. Phys. B* **62**, 39 (1995).
- ¹²R. L. Farrow, D. J. Rakestraw, and T. Dreier, *J. Opt. Soc. Am. B* **9**, 1770 (1992).
- ¹³L. A. Rahn and M. S. Brown, *Opt. Lett.* **19**, 1249 (1994).
- ¹⁴S. Gerstenkorn and R. Luc, *Atlas du Spectre d'Absorption de la Molécule d'Iode* (Editions du CNRS, Orsay, 1979).
- ¹⁵J. Cariou and R. Luc, *Atlas du Spectre d'Absorption de la Molécule de tellure* (Editions du CNRS, Orsay, 1980).
- ¹⁶P. A. Bonczyk and J. A. Shirley, *Combust. Flame* **34**, 253 (1979).
- ¹⁷K. Kohse-Höinghaus, W. Perc, and Th. Just, *Ber. Bunsenges. Phys. Chem.* **87**, 1052 (1983).
- ¹⁸C. F. Kaminski and P. Ewart, *Appl. Phys. B* **61**, 585 (1995).
- ¹⁹B. Attal, D. Debarre, K. Müller-Dethlefs, and J. P. E. Taran, *Rev. Phys. Appl.* **18**, 39 (1983).
- ²⁰T. Dreier and D. J. Rakestraw, *Appl. Phys. B* **50**, 479 (1990).
- ²¹R. L. Abrams and R. C. Lind, *Opt. Lett.* **2**, 94 (1978).
- ²²R. A. Fisher, *Optical Phase Conjugation* (Academic, New York, 1983).
- ²³M. S. Brown, L. A. Rahn, and T. Dreier, *Opt. Lett.* **17**, 76 (1992).
- ²⁴M. Ducloy, F. A. M. de Oliveira, and D. Bloch, *Phys. Rev. A* **32**, 1614 (1985).
- ²⁵B. Grynberg, M. Pinard, and P. Verkerk, *J. Phys.* **47**, 617 (1986).
- ²⁶S. Le Boiteaux, P. Simoneau, D. Bloch, F. A. M. de Oliveira, and M. Ducloy, *IEEE J. Quant. Electron.* **QE-22**, 1986 (1986).
- ²⁷R. P. Lucht, R. L. Farrow, and D. J. Rakestraw, *J.O.S.A. B* **10**, 1908 (1993).
- ²⁸J. F. Lam and R. L. Abrams, *Phys. Rev. A* **26**, 1539 (1982).
- ²⁹E. J. Friedmann-Hill, L. A. Rahn, and R. L. Farrow, *J. Chem. Phys.* **100**, 4065 (1993).
- ³⁰G. Herzberg, *Spectra of Diatomic Molecules*, Vol. 1 of *Molecular Spectra and Molecular Structure* (Van Nostrand Reinhold, New York, 1950).
- ³¹S. Williams, R. N. Zare, and L. A. Rahn, *J. Chem. Phys.* **101**, 1072 (1994).
- ³²S. Williams, R. N. Zare, and L. A. Rahn, *J. Chem. Phys.* **101**, 1093 (1994).
- ³³G. N. Robertson, K. Kohse-Höinghaus, S. Boiteux, F. Aguerre, and B. Attal-Trétout, *J. Quant. Spectrosc. Rad. Transf.* **55**, 71 (1996).
- ³⁴J. Cooper, A. Charlton, D. R. Meacher, P. Ewart, and G. Alber, *Phys. Rev. A* **40**, 5705 (1989).
- ³⁵D. R. Meacher, A. Charlton, P. Ewart, J. Cooper, and G. Alber, *Phys. Rev. A* **42**, 3018 (1990).
- ³⁶P. G. R. Smith and P. Ewart, *Phys. Rev. A* **54**, 2347 (1996).
- ³⁷S. Williams, D. S. Green, S. Sethuraman, and R. N. Zare, *J. Am. Chem. Soc.* **114**, 9122 (1992).
- ³⁸C. Amiot, *Ast. J. Suppl.* **52**, 329 (1983).
- ³⁹R. W. Boyd, *Nonlinear Optics* (Academic, New York, 1992).
- ⁴⁰L. Curtis, B. Engman, and P. Erman, *Phys. Script.* **13**, 270 (1976).
- ⁴¹W. H. Wollaston, *Philos. Trans. R. Soc. Lond.* **11**, 365 (1802).
- ⁴²J. G. Phillips and S. P. Davis, *The Swan System of the C₂ Molecule*, Berkeley Atlas of Molecular Spectra (University of California Press, 1968).
- ⁴³T. Suzuki, S. Saito, and E. Hirota, *J. Mol. Spectros.* **113**, 399 (1985).
- ⁴⁴C. V. V. Prasad and P. F. Bernath, *Astron. J.* **426**, 812 (1994).
- ⁴⁵J. M. Brown, *Program Hund A*.
- ⁴⁶J. M. Brown and A. J. Merer, *J. Mol. Spectros.* **74**, 488 (1979).
- ⁴⁷A. Budó, *Z. Phys.* **96**, 219 (1935).
- ⁴⁸R. L. Farrow, D. J. Rakestraw, and T. Dreier, *J. Opt. Soc. Am. B* **9**, 1770 (1992).
- ⁴⁹R. L. Vander Wal, R. L. Farrow, and D. J. Rakestraw, *24th Symposium (International) on Combustion* (The Combustion Institute, Pittsburgh, PA, 1992).